

## Study of surface photovoltage in hydrogenated amorphous silicon

Shailendra Kumar and S. C. Agarwal

Citation: [Journal of Applied Physics](#) **58**, 3798 (1985); doi: 10.1063/1.335594

View online: <http://dx.doi.org/10.1063/1.335594>

View Table of Contents: <http://scitation.aip.org/content/aip/journal/jap/58/10?ver=pdfcov>

Published by the [AIP Publishing](#)

---

### Articles you may be interested in

[Direct determination of the band-gap states in hydrogenated amorphous silicon using surface photovoltage spectroscopy](#)

Appl. Phys. Lett. **67**, 371 (1995); 10.1063/1.114632

[Surface photovoltage spectroscopy in hydrogenated amorphous silicon](#)

J. Appl. Phys. **65**, 3617 (1989); 10.1063/1.342610

[Light-induced degradation in undoped hydrogenated amorphous silicon films studied by the surface photovoltage technique: A comparison of lifetime versus space-charge effects](#)

J. Appl. Phys. **64**, 1215 (1988); 10.1063/1.341888

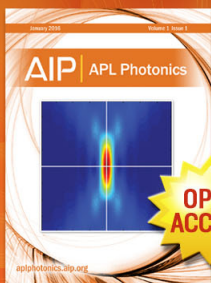
[Improvement in the surface photovoltage method of determining diffusion length in thin films of hydrogenated amorphous silicon](#)

J. Appl. Phys. **61**, 4816 (1987); 10.1063/1.338345

[Surface photovoltage in hydrogenated amorphous silicon](#)

Appl. Phys. Lett. **45**, 575 (1984); 10.1063/1.95286

---



## Launching in 2016!

The future of applied photonics research is here

OPEN  
ACCESS

**AIP** | APL  
Photonics

# Study of surface photovoltage in hydrogenated amorphous silicon

Shailendra Kumar and S. C. Agarwal<sup>a)</sup>

Department of Physics, Indian Institute of Technology, Kanpur 208016, India

(Received 19 February 1985; accepted for publication 14 May 1985)

Surface photovoltage (SPV) in hydrogenated amorphous silicon (*a*-Si:H) has been measured as a function of temperature and wavelength, intensity and chopping frequency of light. Effects of surface treatments on SPV, including etching and exposure to moisture, are also studied. It is concluded that SPV cannot be directly related to the band bending at the surface of *a*-Si:H. By solving Poisson's equation in dark and light, it is shown that in a material such as *a*-Si:H, the observation of a finite SPV necessarily implies a transfer of charge between the surface states and the space-charge region. This explains our experimental observations since it means that SPV measurement may not be relied upon to give the surface potential of *a*-Si:H. Notwithstanding this handicap, it is shown that by measuring SPV and conductance on an *a*-Si:H sample subjected to cycles of moisture and light soaking, we can conclude that light soaking affects the surface as well as the bulk of *a*-Si:H.

## I. INTRODUCTION

The presence of a charged layer at the surface of a semiconductor can be detected from the measurement of surface photovoltage (SPV).<sup>1</sup> The change in the surface potential upon illumination is the measured SPV.<sup>1</sup> If the contribution of the surface states is small, it can be shown that the effect of light is to flatten the bands and thus to reduce the potential at the surface.<sup>2</sup> Thus, in this case, the sign of SPV gives the direction of band bending at the surface. If, however, surface states contribute, Garrett and Brattain<sup>3</sup> have shown that the SPV for low intensity of light can differ from the expected value by a small amount. It has been observed that in crystalline Si,<sup>4</sup> CdS,<sup>5</sup> and InSb,<sup>6</sup> the low-intensity SPV may not give band bending depending upon surface conditions. However, Many *et al.*<sup>7</sup> have argued that at high intensities, the surface potential tends to zero, even if surface states participate, unless some "special surface-state parameters" are involved. Although this statement has been shown to be untrue by Frank and Ulmer,<sup>8</sup> the impression given by Many *et al.*<sup>7</sup> seems to persist, and many SPV measurements at high intensities are done in the hope of finding the surface potential.

Upon shining light, the change in surface potential may be caused by either (i) a redistribution of charge between surface states and the space-charge region, or (ii) a redistribution of charge within the space-charge region without involving surface states, or both. Since charge neutrality requires that the charge in surface states ( $Q_{ss}$ ) should be equal and opposite to space charge ( $Q_{sc}$ ),

$$Q_{ss} + Q_{sc} = 0.$$

For processes described in (i) the change in  $Q_{sc}$ ,  $\Delta Q_{sc} = -\Delta Q_{ss}$  and for (ii)  $\Delta Q_{sc} = 0$ .

Johnson<sup>2</sup> gave a theory of SPV at high injection levels and developed a method of graphical analysis to show how the surface potential changes under illumination. His analysis shows that light injection tends to decrease the band bending, i.e., flatten the bands for process (ii), but may or

may not do so for process (i) where the space charge changes. In the case of crystalline Ge and Si, the analysis implies that at high intensities, SPV will directly give the band bending within  $1 kT/e$ , if process (ii) dominates.

Clearly, if it can be ensured that  $Q_{sc} = 0$  in light (i.e.,  $\Delta Q_{sc} = -Q_{sc}$ ), the observed SPV will be equal to the surface potential even in case (i). However, this cannot always be guaranteed and the observed SPV can be either positive or negative depending on the ratio of the capture rates for electrons and holes of surface states.<sup>6,8</sup> In the case of hydrogenated amorphous silicon (*a*-Si:H), Fritzsche<sup>9</sup> has argued that  $Q_{sc}$  most probably is not zero in the presence of light because the charges may be separated too far spatially and energetically to equilibrate.

In spite of this complication, surface photovoltage measurements on a *a*-Si:H have been carried out in several laboratories.<sup>10-12</sup> It has been difficult to interpret the results in a straightforward manner<sup>11-12</sup> and there is evidence to suggest<sup>13</sup> that SPV measurements are not useful in obtaining the band bending at the surface of *a*-Si:H.

In the present work, Johnson's graphical analysis<sup>2</sup> is applied for *a*-Si:H, considering a continuous distribution of localized states in the mobility gap. In Sec. II, a relation between the space-charge density ( $Q_{sc}$ ) and the surface potential ( $V_s$ ) is derived in dark and in presence of light, by solving Poisson's equation for  $V_s$ . It is shown that in *a*-Si:H, process (ii) gives negligible SPV and a change in  $Q_{sc}$  is necessary [i.e., process (i)] to observe a finite SPV. In Sec. III, the method of measurement of SPV using pulsed light is described. In Sec. IV, the effects of repetition frequency ( $f$ ), intensity ( $I$ ), and energy ( $h\nu$ ) of the pulsed light are discussed. Effects of etching, aging, and ambient air on SPV have also been studied. In addition, SPV at the free surface and the film substrate interface has been measured as a function of temperature. These measurements show that the SPV does not give band bending. This supports the theoretical results of the Sec. II, since finite SPV means a change in  $Q_{sc}$  for *a*-Si:H and therefore surface state parameters are expected to govern the SPV. In the last section, the effect of light soaking (Staebler-Wronski effect)<sup>14</sup> on SPV is described. In this ex-

<sup>a)</sup> At present, visiting Energy Conversion Devices, Inc., 1675 West Maple Road, Troy, Michigan 48064.

periment, samples are exposed to a sequence of light soaking and moisture similar to Tanielian.<sup>15</sup> However, in addition to the dark conductance ( $G$ ), the SPV is also measured. It is observed that the SPV is sensitive to the sequence of illumination and moisture. From these measurements, it is concluded that the light soaking changes the surface as well as the bulk states in  $\alpha$ -Si:H.

## II. THEORY OF SURFACE PHOTOVOLTAGE

In this section, we give a graphical method similar to that of Johnson<sup>2</sup> to obtain SPV in  $\alpha$ -Si:H.

### A. Solution of Poisson's equation in dark and light

The energy band diagram, in presence of light, for an undoped sample with an accumulation layer is shown in Fig. 1. In bulk,  $E_c$  and  $E_v$ , respectively, are the conduction-band and valence-band mobility edges,  $E_f$  is the Fermi energy level in dark,  $E'_{fn}$  and  $E'_{fp}$  are the quasi Fermi levels for trapped electrons and holes, respectively, in light. In the space-charge region, the electrostatic potential  $V(x)$  at the point  $x$  is positive for downward band bending and energy level ( $E$ ) is shifted by an energy ( $-eV$ ),  $e$  being the magnitude of the electronic charge. It is well known that there is a continuous distribution of localized states in the mobility gap of  $\alpha$ -Si:H.<sup>16</sup> We estimate the density of states between  $10^{16}$  and  $10^{17} \text{ cm}^{-3} \text{ eV}^{-1}$  at the Fermi level in our undoped samples.<sup>17</sup> Using Shockley-Read statistics,<sup>18</sup> Simmons and Taylor<sup>19</sup> have derived the occupation probability of an energy level lying in the mobility gap in nonequilibrium conditions. For convenience, it is assumed that the quasi Fermi levels are flat up to the surface. The traps are monovalent, and those existing below  $E_f$  are neutral when filled with an electron and that the traps positioned above  $E_f$  are neutral when empty. Furthermore, assuming that the ratio  $R$  of the capture rates for electrons and holes is constant for all energy levels, the probability of occupation  $f(E, E'_{fn})$ , of an energy level  $E$  above  $E_f$  by an electron is<sup>19</sup>

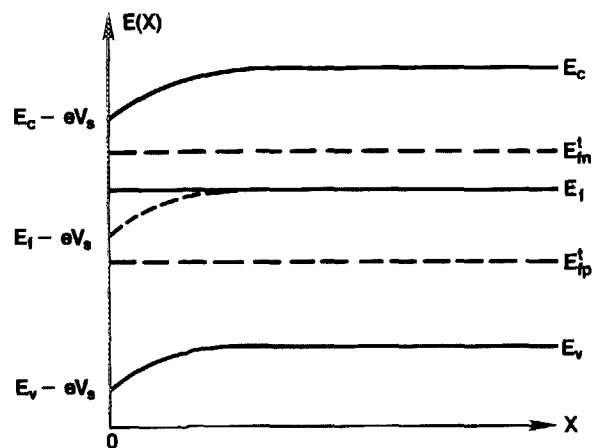


FIG. 1. Energy band diagram for  $\alpha$ -Si:H with an accumulated surface in light.  $E_c$  and  $E_v$  are mobility edges,  $E_f$  is the Fermi level in dark.  $E'_{fn}$  and  $E'_{fp}$  are quasi Fermi levels for trapped carriers. Potential  $V$  is positive and energy level  $E$  in bulk is shifted to  $E - eV_s$  at the surface.

$$f(E, E'_{fn}) = \frac{Rn_b}{Rn_b + p_b} \frac{1}{1 + \exp[(E - E'_{fn})/kT]}, \quad (1)$$

where  $n_b$  and  $p_b$  are the free electron and hole densities in the bulk, and the probability of occupation of an energy level below  $E_f$  by a hole is

$$1 - f(E, E'_{fp}) = \frac{p_b}{Rn_b + p_b} \frac{1}{1 + \exp[-(E - E'_{fp})/kT]} \quad (2)$$

The potential  $V(x)$  at a distance  $x$  from the surface satisfies the Poisson's equation

$$\nabla^2 V(x) = -\rho(x)/\epsilon, \quad (3)$$

where  $\rho(x)$  is the effective charge density and  $\epsilon$  is the permittivity of the medium.

Charge density  $\rho(x)$  is given by

$$\begin{aligned} \rho(x) = e \int_{-\infty}^{E_v} g(E) [f(E, E'_{fp}) - f(E, E'_{fp} + eV)] dE \\ + \int_{E_v}^{E_f} g(E) [f(E, E'_{fp}) - f(E, E'_{fp} + eV)] dE \\ + \int_{E_f}^{E_c} g(E) [f(E, E'_{fn}) - f(E, E'_{fn} + eV)] dE \\ + \int_{E_c}^{\infty} g(E) [f(E, E'_{fn}) - f(E, E'_{fn} + eV)] dE, \end{aligned} \quad (4)$$

where  $E'_{fn}(E'_{fp})$  and  $E_{fp}(E'_{fn})$  are the quasi Fermi levels for free (trapped) electrons and holes, respectively, and  $g(E)$  is the distribution of density of states. In Eq. (4), the first and the fourth integrals give contribution to the density of free carriers ( $\rho_0$ ) due to holes and electrons, respectively, and the second and the third integrals represent the density ( $\rho_t$ ) of trapped holes and electrons, respectively. For convenience, these integrals are denoted by  $I_1$ ,  $I_2$ ,  $I_3$ , and  $I_4$ , respectively. These can be evaluated using Eqs. (1) and (2) and the standard Fermi distributions  $f(E, E'_{fp})$  and  $f(E, E'_{fn})$  for free carriers.  $g(E)$  below and above the valence and conduction-band mobility edges is taken to be  $g(E_v)$  and  $g(E_c)$  for  $I_1$  and  $I_4$ , respectively; and a constant density of states  $g(E) = g_0$  is chosen for  $I_2$  and  $I_3$ . With these assumptions, the integrals can be carried out and are given by

$$I_1 = p_b [\exp(-v) - 1], \quad (5)$$

$$I_4 = n_b [1 - \exp(v)], \quad (6)$$

$$\begin{aligned} I_2 = \frac{kTg_0p_b}{Rn_b + p_b} \ln \frac{1 + \exp[-\beta(E_v - E'_{fp})]}{1 + \exp[-\beta(E_v - E'_{fp}) + v]} \\ \times \frac{1 + \exp[\beta(E'_{fp} - E_f) + v]}{1 + \exp[\beta(E'_{fp} - E_f)]}, \end{aligned} \quad (7)$$

and

$$\begin{aligned} I_3 = \frac{kTg_0Rn_b}{Rn_b + p_b} \ln \frac{1 + \exp[-\beta(E_c - E'_{fn}) - v]}{1 + \exp[\beta(E_c - E'_{fn})]} \\ \times \frac{1 + \exp[\beta(E_f - E'_{fn})]}{1 + \exp[\beta(E_f - E'_{fn}) - v]}, \end{aligned} \quad (8a)$$

where

$$\beta \equiv 1/kT \text{ and } v \equiv eV/kT.$$

These integrals hold good both in light and in dark. In dark, one puts  $E_f = E'_{fn} = E'_{fp}$  and uses dark values of  $n_b$  and  $p_b$ . To evaluate  $I_3$  and  $I_4$  in light, information about the quasi Fermi levels for the trapped charges is necessary. Assuming that the quasi Fermi levels for free carriers are the same as for the trapped carriers ( $E'_{fn} = E_{fn}$ ,  $E'_{fp} = E_{fp}$ ), one can estimate the positions of the quasi Fermi levels from the photoconductivity data. Let us estimate them for a high intensity which gives a photoconductivity which is 4 orders of magnitude larger than the dark conductivity. For an undoped sample, with activation energy  $E_o = 0.65$  eV and band gap  $E_G = 1.6$  eV, we obtain

$$E_c - E'_{fn} = 0.4 \text{ eV}; E'_{fn} - E_f = 0.25 \text{ eV}. \quad (8b)$$

Other energy differences are calculated assuming  $E_c - E_{fn} = E_{fp} - E_v$ . This will be true if light creates an equal number of free electrons and holes. Although, in reality, the free hole concentration is likely to be smaller,<sup>20</sup> this assumption is not likely to change the conclusions in a qualitative manner.

Using these energy differences and neglecting appropriate terms, the trapped charge density will be

$$\rho_t(x) = -e g_o kT v(x). \quad (9)$$

Although, Eq. (9) is derived for high intensity of light, it also holds good in dark because it is independent of the position of the quasi Fermi levels. It may be interesting to note that the  $\rho_t(x)$  given by Eq. (9) is the same when Fermi distributions are approximated by a step function using zero-temperature statistics.<sup>9</sup> Poisson's equation becomes

$$\left(\frac{e}{kT}\right)^{-1} \frac{d^2 v(x)}{dx^2} = -[\rho(x)/\epsilon] = (e/\epsilon) \times [n_b(e^v - 1) - p_b(-e^{-v} + 1) + g_o kT v(x)]. \quad (10)$$

This yields

$$(dv/dx)^2 = -(2e/\epsilon kT) \int \rho(x) dv, \quad (11)$$

and the space-charge density (per unit area)  $Q_{sc}$  is given by Gauss's law,

$$Q_{sc} = \pm |dV/dx|, \quad (12)$$

where the positive sign is for negative  $V$  and vice versa. Using Eqs. (11) and (12), the charge per unit area is given by

$$Q_{sc} = \pm (2e\epsilon \{ n_b [\exp(v_s) - v_s - 1] - p_b [\exp(-v_s) + v_s - 1] + g_o kT v_s^2/2 \})^{1/2}. \quad (13a)$$

The corresponding expression for the case of constant impurity concentration and complete ionization in a crystalline semiconductor<sup>7</sup> is

$$Q_{sc} = \pm (2e\epsilon \{ n_b [\exp(v_s) - v_s - 1] - p_b [\exp(-v_s) + v_s - 1] \})^{1/2}. \quad (13b)$$

It may be noted that Eqs. (13) have been derived for all intensities of light, assuming a constant density of states, an approximation which becomes worse for *a*-Si:H, as one moves

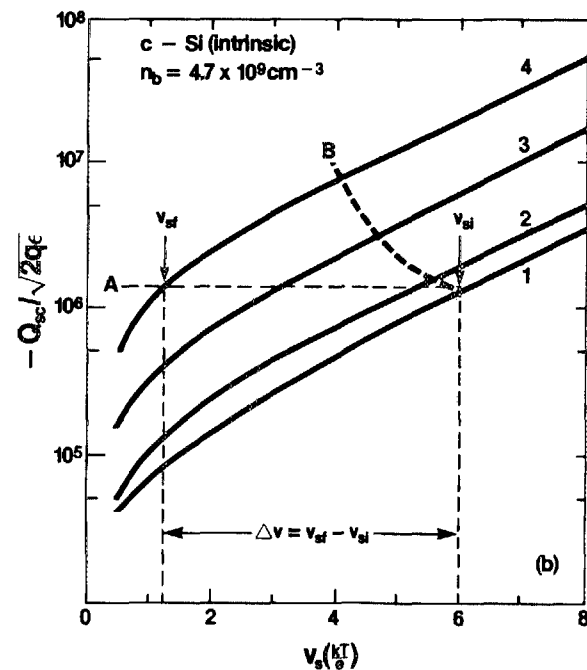
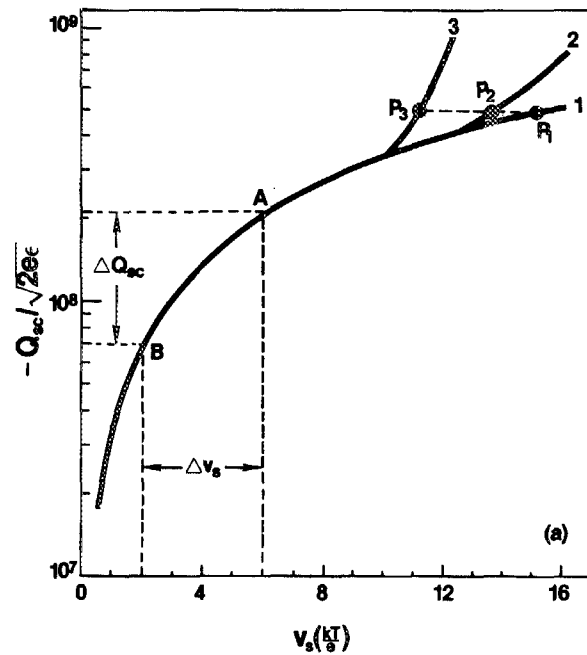


FIG. 2. (a) Space-charge density  $Q_{sc}$  vs surface potential  $v_s$  for *a*-Si:H with negative space-charge region in dark (1) and light [(2)  $\Delta n_b = 5 \times 10^{10} \text{ cm}^{-3}$  and (3)  $\Delta n_b = 5 \times 10^{11} \text{ cm}^{-3}$ ].  $v_s$  is in units of  $(kT/e)$ . (b) Space-charge density  $Q_{sc}$  vs surface potential  $v_s$  for *c*-Si (intrinsic) with negative space-charge region in dark (1) and light [(2)  $\Delta n_b = 10^{10} \text{ cm}^{-3}$ ; (3)  $\Delta n_b = 10^{11} \text{ cm}^{-3}$ ; (4)  $\Delta n_b = 10^{12} \text{ cm}^{-3}$ ].

towards the band edges. However, for the Fermi-level shift of the kind indicated in Eq. (8b), the variation in  $g(E)$  between the dark and quasi Fermi levels is likely to be small, especially for our samples, having  $g(E_F) \approx 10^{17} \text{ cm}^{-3} \text{ eV}^{-1}$ .

## B. Graphical analysis of SPV

Figure 2(a) shows the graphical plot of Eq. (13a) in dark (curve 1), and, for medium and high illuminations (curves 2 and 3, respectively), for an undoped *a*-Si:H sample, having

an accumulated surface, with  $g_0 = 10^{17} \text{ cm}^{-3} \text{ eV}^{-1}$  and activation energy  $E_a = 0.65 \text{ eV}$ . In dark,  $n_b = 5 \times 10^8 \text{ cm}^{-3}$  and  $p_b = 5 \times 10^3 \text{ cm}^{-3}$ .  $n_b$  and  $p_b$  increase to  $n_b + \Delta n_b$  and  $p + \Delta p_b$ , respectively, in the presence of light. For the high-intensity curve 3 in Fig. 2(a), we have chosen  $\Delta n_b = 5 \times 10^{12} \text{ cm}^{-3}$  which corresponds to a change by about 4 orders of magnitude in conductivity upon shining light. Curve 2 is for  $\Delta n_b = 5 \times 10^{10} \text{ cm}^{-3}$ . Further, for the sake of simplicity,  $\Delta p_b$  has been taken to be equal to  $\Delta n_b$ . As mentioned earlier, this need not be true, but will not affect the conclusions drawn here. The corresponding curves for the depleted surface are obtained simply by changing the signs of  $Q_{sc}$  and  $v_s$  in Fig. 2(a).  $Q_{sc}$  vs  $v_s$  curves calculated using Eq. (13b) for *c*-Si (intrinsic) with an electron accumulation layer are shown in Fig. 2(b). Curve 1 is for dark ( $n_b = p_b = 4.7 \times 10^9 \text{ cm}^{-3}$ ). Curves 2, 3, and 4 are for progressively increasing light intensities, and are shifted to the left of the curve 1 for all values of  $v_s$ , even for the very small intensities of light. In contrast, for *a*-Si:H, curves 2 and 3 in Fig. 2(a) under illumination coincide with curve 1 in dark up to  $v_s = 10$ . This difference between *c*-Si and *a*-Si:H arises primarily because the latter has  $\rho_0 \ll \rho_i$  and has been assumed to have a constant density of localized states. For a low-defect density material [ $g(E_F) \approx 5 \times 10^{15} \text{ cm}^{-3} \text{ eV}^{-1}$ ], however, the assumption of constant density of states is not likely to hold, and Eq. (13a) must be replaced by a more complicated relation which depends on the distribution of localized states. For a slowly rising  $g(E)$ , a small shift of curve 1 to the left is expected upon shining light.

In the case of *c*-Si, using light pulses of appropriate frequency, it has been possible to keep the  $Q_{ss}$  and hence the  $Q_{sc}$  constant during the experiment.<sup>21</sup> In this case, the system in Fig. 2(b) moves along a horizontal line. The line A applies to a particular case, where initial  $v_{si}$  in dark is 6. The values of the surface potential for different intensities of light are described by the intersections of line A with the  $Q_{sc}$  curves. The quantity  $\Delta v = v_{sf} - v_{si}$  is the photovoltage. At high enough intensities,  $V_{sf}$  is close to zero and the observed SPV is equal to the band bending at the surface in dark to within  $\sim (kT/e)$ . If  $Q_{ss}$  changes during the injection, the system will move along a path other than A (on the line B, for example,) giving a different  $\Delta v$ . The path of the system will depend upon the properties of surface states. In fact,  $\Delta v$  could be zero or even change sign depending upon the path followed by the system. Experimentally, in the case of *c*-Si<sup>21</sup> and *c*-Ge,<sup>2</sup> it has been observed that the large-signal surface photovoltage is not very sensitive to fast surface states. Therefore, SPV measurement with high-intensity light and at frequencies high enough to suppress the contribution from the slow states, is a fairly reliable tool for determining the surface potential in these cases. However, for small-signal SPV measured at low frequencies, the contribution from surface states does not appear to be negligible as compared to the contribution from the redistribution within the space charge. It has been observed in the case of crystalline Si that the SPV may not be zero even if  $v_s = 0$ .<sup>4,8</sup>

Let us now consider SPV in *a*-Si:H. In Fig. 2(a), the curves 2 and 3 under illumination coincide with curve 1 in dark up to  $v_s = 10$ . Now, if the surface states do not partici-

pate,  $Q_{sc}$  remains constant upon shining light. Let the system be at  $P_1$  on the curve 1 in dark. In light, the system moves along a horizontal line intersecting curves 2 and 3 at  $P_2$  and  $P_3$ , respectively. The expected SPV is then surface potential difference between  $P_1$  and  $P_2$  for  $\Delta n_b = 5 \times 10^{10} \text{ cm}^{-3}$  and between  $P_1$  and  $P_3$  for  $\Delta n_b = 5 \times 10^{12} \text{ cm}^{-3}$ .

Clearly, if  $v_s$  in dark is less than 10 (which is normally the case for *a*-Si:H),<sup>22</sup> this procedure will predict a zero SPV since curves 1, 2, and 3 overlap. Furthermore, the observed SPV in *a*-Si:H is not zero (and is in fact more than 100 mV in some cases), we must question our assumption that  $Q_{sc}$  is unchanged and the system moves along a horizontal line. A significant change in  $Q_{sc}$  can occur only by exchanging charges with the surface states, since the density of free carriers for  $|v_s| < 10$  is too small. Therefore, for a change in  $Q_{sc}$  by an amount  $\Delta Q_{sc}$ , the surface states charge  $Q_{ss}$  must change by  $\Delta Q_{ss} = -\Delta Q_{sc}$ . In that case, the system need not move in a horizontal line and the observation of a large SPV can be explained. For example, if in dark, the system is at A [see Fig. 2(a)], corresponding to  $v_s = 6$ , it can move to B, and give  $\text{SPV} = 4kT/e$ , if we allow for a change in  $Q_{sc}$ .  $\Delta Q_{sc} \approx 1.5 \times 10^8 \sqrt{(2e\epsilon)}$  Coulomb upon shining light. Since the dark and illuminated curves coincide in this region, the path of the system from A to B must not deviate from this curve in this case. It is interesting to note that  $\Delta Q_{sc}$  may be positive or negative depending on the nature of surface states, and so the observed photovoltage could even be of opposite sign for the same initial value of  $v_s$ . For the example cited above,  $\text{SPV} = 4kT/e$  ( $\approx 100 \text{ mV}$  at  $T = 300 \text{ K}$ ),  $\Delta Q_{ss} = 10^{-8} \text{ C}$  and this gives a surface states density of  $\approx 10^{11} \text{ cm}^{-2}$ , participating in the charge transfer. This number is quite reasonable and agrees with other measurements of surface states density.<sup>15,22</sup>

Thus we are led to the following conclusion. For reasonable values of the surface potential (i.e., less than  $10kT/e$ ) in *a*-Si:H, the SPV will be zero for the process (ii) (i.e.,  $\Delta Q_{sc} = 0$ ). If finite SPV is observed, process (i) must dominate, which means that the surface states must participate. One expects that for higher chopping frequencies,  $\Delta Q_{ss}$  will be smaller and hence the magnitude of SPV will go down as the chopping frequency is increased.

### III. EXPERIMENT

The experimental setup used for measuring SPV is shown in Fig. 3(a). *a*-Si:H samples deposited on Corning 7059 glass substrates, and of thickness 0.6–1.5  $\mu\text{m}$ , having two nichrome electrodes 1 and 2 with a gap of 1–1.8 cm are used. To measure SPV at the front surface of the sample, a semitransparent ( $\approx 100 \text{ \AA}$  gold on 7059 glass) electrode (3) is kept at a distance of 0.1 mm from the semiconductor surface. Electrode (3) is insulated from electrodes (1) and (2) by Teflon tape. Pulses of light (fwhm = 3  $\mu\text{s}$ , repetition frequency 2.5 Hz  $< f < 450 \text{ Hz}$ ) are allowed to fall on the sample through the semitransparent electrode. Illumination of the sample causes charge rearrangement, and the induced voltage is picked up by the semitransparent electrode. This signal is fed into a high input impedance buffer circuit before displaying on an oscilloscope (CRO). Appropriate light filters are used

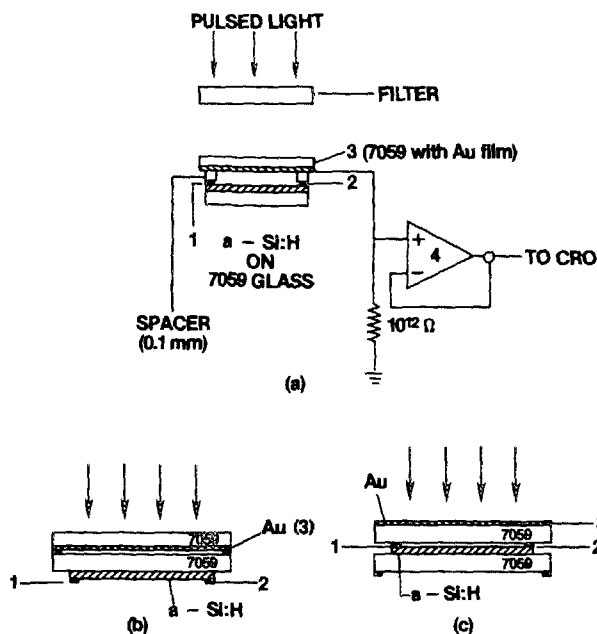


FIG. 3. (a) Arrangement for the measurement of SPV. 3 is a semitransparent gold electrode. Electrodes 1 and 2 are for measurement of  $G$  and are grounded for SPV measurements. 4 is a FET input operational amplifier. (b) Geometry used to measure SPV at the back surface. (c) Geometry used to measure SPV at the front surface, keeping separation between electrode 3 and the sample same as in (b).

to vary the energy of the pulsed light between 1.8 and 3 eV. Neutral density filters are used to vary the intensity.

Most of the measurements on the free surface are done using the geometry shown in Fig. 3(a). To compare SPV at the free surface and the film substrate interface in identical conditions, the geometry shown in Figs. 3(b) and 3(c) is used. To calibrate the system,<sup>2,4</sup> square wave pulses of frequency between 2.5 and 400 Hz are fed to a gold film kept in place of the sample. For the geometry used in Fig. 3(a), the input signal reduces by a factor of 2.9 and for geometries used in Figs. 3(b) and 3(c), it is reduced by a factor of 3.4 for all frequencies. SPV results measured in different geometries are corrected by appropriate calibration factors.

#### IV. EXPERIMENTAL RESULTS

SPV, on heat-dried samples (i.e., annealed in vacuum at 150 °C for 2 h), is measured with varying chopping frequency ( $f$ ), intensity ( $I$ ), and energy ( $h\nu$ ) of the pulsed light. Although most of the time SPV is measured by keeping the electrodes (1) and (2) (Fig. 3) in dark, the results are unaffected if they are exposed to light. In the following, the values of SPV quoted are the peak heights (during light pulse) of SPV observed as time-dependent signals on the CRO.

##### A. Frequency dependence

Variation of SPV with repetition frequency ( $f$ ) of the pulses is shown in Fig. 4(a). For convenience,  $f$  is plotted on a logarithmic scale and SPV on a linear scale. SPV is positive for all values of  $f$  between 2.5 Hz to 400 Hz. For  $f < 4$  Hz, SPV is almost constant and for higher frequencies, it decreases logarithmically. SPV, due to one pulse, takes typically about 250 ms to decay. At higher frequencies, SPV, due to

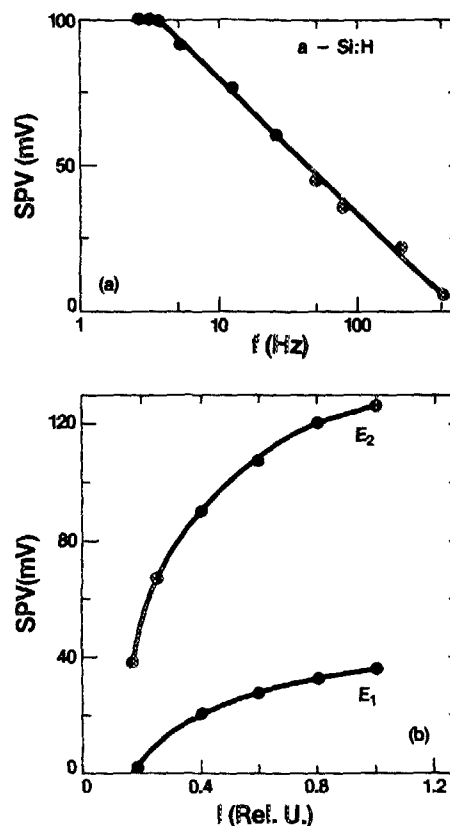


FIG. 4. (a) SPV as a function of repetition frequency ( $f$ ) of pulsed light on the front surface of  $\alpha$ -Si:H sample. (b) SPV as a function of intensity ( $I$ ) of the pulsed light for optical gap light  $E_1$  and high-energy light  $E_2$ .

the next pulse, overlaps with the decaying SPV signal from the previous pulse. Moreover, at lower frequencies slower states can also contribute to SPV.

##### B. Dependence upon intensity and energy of light

Figure 4(b) shows a variation of SPV as a function of the intensity of light for two filters (allowing light of energy 1.6 eV  $< E_1 < 1.8$  eV and 2 eV  $< E_2 < 2.8$  eV, respectively) measured on the free surface. For the band-gap light ( $E_1$ ) as well as the high-energy light ( $E_2$ ) SPV shows saturation at high intensities. One might try to explain this as being caused by the Dember effect.<sup>7</sup> The Dember potential arises from the potential gradient set up internally to equalize the otherwise different electrons and hole diffusion currents in the direction of the incident light.<sup>7</sup> This takes place because of the difference in the mobilities of electrons and holes. This effect is negligible in a uniformly excited sample.<sup>7,23</sup> Optical band-gap light  $E_1$  gives a uniform excitation of the sample, whereas  $E_2$  gets absorbed near the front surface. Thus if the Dember effect were large, it could explain the difference. But this is not likely, since among other things, the geometry of the electrodes used is not favorable for the Dember effect. We have, however, a simpler explanation for this behavior of SPV with  $E$ . Since the band-gap light ( $E_1$ ) sees the front as well as the back surface, the measured SPV will be the algebraic sum of the contributions from the front and the back, whereas the contribution to the SPV from the high-energy light ( $E_2$ ) comes primarily from the surface on which it is

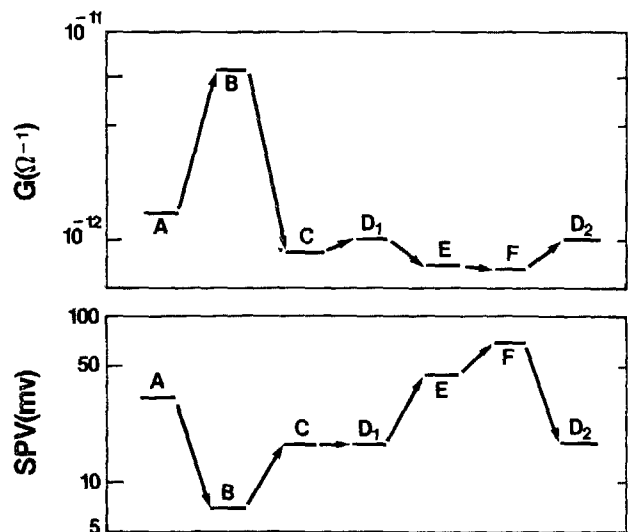


FIG. 5. Upper and lower parts show, respectively, the conductance ( $G$ ) and SPV after different surface treatments of an  $\alpha$ -Si:H sample. A: nonetched, heat dried measured in vacuum; B: etched, measured in air; C: state B measured in vacuum,  $10^{-5}$  Torr;  $D_1$ : after heat-drying C, measured in vacuum; E: heat dried after 15 days of  $D_1$ , measured in vacuum; F: heat dried after 30 days of  $D_1$ , measured in vacuum;  $D_2$ : after etching, heat drying F, measured in vacuum.

shone. SPV is measured at the highest intensity by shining  $E_2$  at the back of the sample. It is found to be 70 mV. This shows that SPV at front is larger (125 mV) than at the back (70 mV). For  $E_1$ , we expect 55 mV and  $-55$  mV at the front and the back, respectively. These are not very different from the measured values of 36 mV and  $-40$  mV, respectively, considering the qualitative nature of this simple explanation. This behavior for low and high energies is observed for all samples. Unless otherwise specified, high-energy light  $E = 3$  eV is used for the measurements of SPV reported here, in order to avoid interference from the back surface.

### C. Effect of etching, aging, and ambient

SPV and conductance have been measured to check the effect of etching, aging, and ambient air on the free surface of  $\alpha$ -Si:H samples. Light of energy  $E = 3$  eV and pulsed frequency  $f = 2.5$  Hz is used to measure SPV. Figure 5 shows the dark conductance ( $G$ ) and SPV measured in different states of a sample, produced by etching, heat drying, aging, and varying ambient. A heat-dried sample (annealed in vacuum at  $150^\circ\text{C}$ , 2 h) measured in vacuum is represented by the state A ( $G = 1.45 \times 10^{-12} \Omega^{-1}$  and  $\text{SPV} = 32$  mV). The etched sample (etched for 5 min in 10% HF and cleaned by deionized water and vapors of isopropyl alcohol) measured in air is given by the state B ( $G = 1.1 \times 10^{-11} \Omega^{-1}$ ;  $\text{SPV} = 7$  mV). After this the system is evacuated (state C) and  $G$  reduces to  $8.5 \times 10^{-13} \Omega^{-1}$  and SPV increases to 17 mV. Now the sample is heat dried and the state  $D_1$  ( $G = 10^{-12} \Omega^{-1}$  and  $\text{SPV} = 17$  mV) is reached. The sample is kept in a dessicator for 15 days. It is heat dried (State E) and measured ( $G = 7 \times 10^{-13} \Omega^{-1}$ ,  $\text{SPV} = 46$  mV). The process is repeated after 30 days and we obtain the state F ( $G = 6.8 \times 10^{-13} \Omega^{-1}$ ,  $\text{SPV} = 70$  mV). Etching and heat drying the sample in state F brings it to the state  $D_2$  which is the same as the state  $D_1$ .

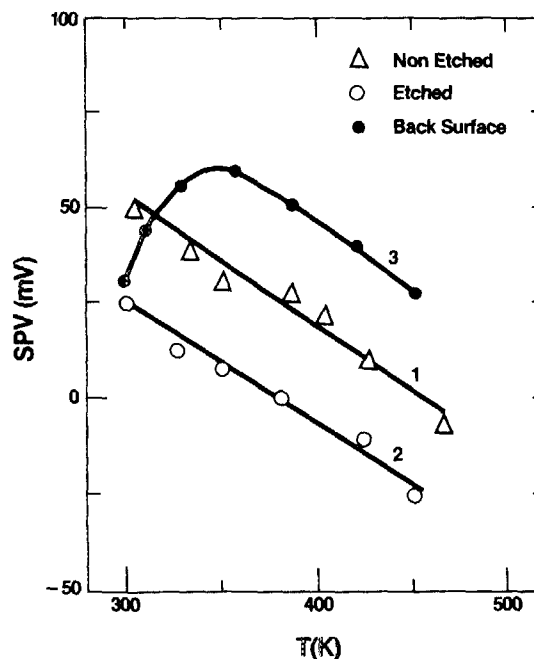


FIG. 6. SPV as a function of  $T$  for an  $\alpha$ -Si:H sample. Curve 1: nonetched and heat-dried front surface; Curve 2: etched and heat-dried front surface; and Curve 3: heat-dried back surface.

### D. Temperature dependence

Figure 6 shows the SPV at the free surface and at the film substrate interface as a function of temperature ( $T$ ) between 300 and 450 K. Curves (1) and (2) are for the free surface, before and after etching, respectively. Curve (3) is the SPV for the back surface. All measurements are done after heat drying. For nonetched front surface (Curve 1), SPV is positive at room temperature, decreases linearly at higher temperatures, and finally becomes negative at  $T = 460$  K. After etching and heat drying, it reduces at room temperature (300 K), but remains positive. It changes sign at  $T = 380$  K and becomes more negative at higher temperatures (Curve 2). The temperature dependence of SPV at the back surface is quite different than at the free surface. It remains positive in the whole temperature range and shows a peak at about 350 K (Curve 3). It increases between  $T = 300$  and 350 K and then decreases linearly at higher temperatures.

The temperature dependence of SPV at the back surface is almost the same for all samples. However, although the shape of SPV vs  $T$  plot for the front surface remains unchanged from sample to sample, the magnitude of SPV shows a variation. It seems to depend on the sample history.

### V. INTERPRETATION

In the case of crystalline semiconductors, repetition frequency of pulsed light is usually chosen such that the charge in the surface states does not have time to change during illumination.<sup>2,18</sup> Since overall neutrality must be preserved, injected carriers cannot produce a net charge change in the space charge, but instead will cause a charge redistribution. In this situation, as discussed in Sec. II, the light injection



reduces surface potential, i.e., the light tends to flatten the bands.

So, in principle, it is possible to determine the direction as well as magnitude within a  $kT/e$  from the saturated value of SPV using high-intensity excitation.<sup>7</sup> However, as discussed in Sec. II, the situation becomes complex if charge exchange takes place between surface states and the space-charge region. In this case, the SPV may not be relied upon to give the sign and the magnitude of surface potential. Other contributions to the measured SPV may originate from a photovoltage generated at the metal semiconductor contact (contact photovoltage) and from the Dember effect.<sup>7</sup> However, in the present case, these contributions turn out to be small, as discussed in Sec. IV B.

### A. Frequency dependence

In Fig. 4(a), SPV is larger for lower frequencies. This can be explained by the fact that at lower frequencies more surface states (i.e., slower ones) can contribute to the charge transfer. At higher frequencies, the contribution from the surface states reduces, and one gets a situation of almost constant  $Q_{sc}$  near 1 kHz. The observation that the SPV tends to zero as  $f$  increases supports the theoretical results (Sec. II). Also, the SPV reaches its maximum saturation value for  $f < 4$  Hz. This shows that there are very few surface states with time constant  $> 1$  s or  $< 1$  ms, which contribute to SPV. SPV at low frequencies necessarily involves a transfer of charge between surface states and the space-charge region [i.e., process (i) in Sec. I].

### B. Intensity dependence

If one assumes a reasonable band bending in dark (e.g.,  $v_s = 6 kT/e$ ), it is possible to find out the charge transfer upon shining light. Using the  $Q_{sc}$  vs  $v_s$  curve Fig. 2(a), the saturated value of SPV at high intensity implies a density of about  $10^{11} \text{ cm}^{-2}$  surface states. Similar values are reported by others as well.<sup>15,22</sup>

### C. Change in surface conditions

Different surface treatments described in Sec. IV C are likely to change the surface potential  $v_s$ , resulting in a change in  $G$  and SPV. The conductance ( $G$ ) measured in a coplanar geometry is a function of the surface potential and is given by<sup>9</sup>

$$G = \frac{w}{l} \sigma_0 \int_0^t \exp \left( \frac{-(E_c - E_f)}{kT} + \frac{eV(x)}{kT} \right) dx, \quad (14)$$

where  $w$  is the length of the electrodes and  $l$  is the separation between them,  $t$  is the thickness of the sample, and  $V(x)$  is the potential in the space-charge region. As an example, we estimate the maximum possible change in  $G$ , if  $V_s$  changes from  $-0.1 \text{ eV}$  to  $+0.1 \text{ eV}$ , for a sample of thickness  $t = 1.0 \mu\text{m}$  having the width of the space-charge region  $\approx 0.2 \mu\text{m}$ , in both accumulated and depleted surface conditions. Exact information about the potential distribution and its variation with surface potential is required to calculate the dependence of  $G$  on surface potential ( $V_s$ ). In the absence of any information about the potential distribution in the space-

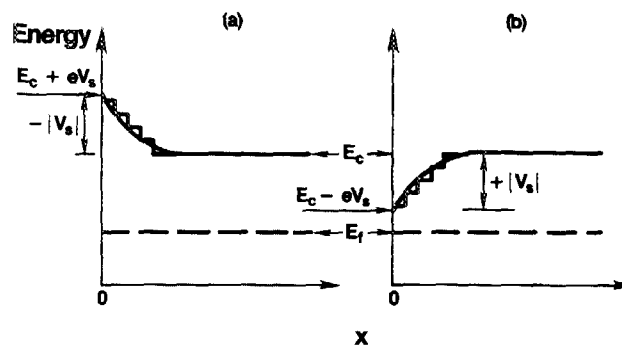


FIG. 7. Energy band diagram (a) with upward band bending at the surface and (b) with downward band bending at the surface, broken in small steps for the calculation in the text.

charge region, we use the following approximate method for our calculation. Let us divide the space-charge region in four strips, each of thickness  $0.05 \mu\text{m}$  as shown in Fig. 7. The potential drop from one strip to another is  $0.025 \text{ V}$ . Using Eq. (14) for  $G$ , one gets  $G(V_s = 0.1 \text{ V})/G(V_s = -0.1 \text{ V}) \approx 5$ . Therefore, for a change in  $V_s$  from  $-0.1 \text{ V}$  to  $+0.1 \text{ V}$ , an increase in  $G$  by about a factor of 5 is expected.

Let us try to understand the results of Fig. 5 giving  $G$  and SPV after different surface treatments in terms of the change in  $V_s$ . Since high-intensity SPV, in some cases, does give the surface potential,<sup>7</sup> let us assume for the sake of argument that it does so for  $a\text{-Si:H}$  also. We shall show that the results cannot be explained in this manner.

Since the SPV is positive in all states (Fig. 5), the bands must bend upwards as per our assumption.  $G$  increases by a factor of 7 in going from the state  $A$  to the state  $B$ . Starting from any reasonable value of  $V_s$  in state  $A$ , this increase in  $G$  would imply a downward band bending in the state  $B$ , as estimated using procedure outlined above. Therefore, one expects a negative SPV in state  $B$ . But the observed SPV in this state is positive ( $+7 \text{ mV}$ ). Furthermore, the increase in SPV by  $10 \text{ mV}$  from the state  $B$  to the state  $C$  is too small to explain the large (by a factor more than 10) decrease in  $G$ . The discrepancy is even more striking if we compare the state  $A$  with the state  $C$ . Both  $G$  and SPV in state  $A$  are larger than the state  $C$ . Since SPV is positive and assumed to give upward band bending, this (SPV) implies that the state  $A$  has more upward bending of bands than the state  $C$ . But then  $G$  for the state  $A$  should have been smaller than that of the state  $C$ . Thus, the results cannot be understood if SPV were to give the band bending at the surface.

The measured SPV and  $G$  in states  $D_1$ ,  $E$ , and  $F$  (Fig. 5) are also inconsistent with the hypothesis that SPV gives band bending. In this case, since heat drying and aging are involved, one could argue that these may change the bulk states as well. But upon etching and heat drying the sample in state  $F$ , state  $D_1$  is reproduced. Since the sample was heat dried to start with and was heat dried at several other stages, namely  $D_1$ ,  $E$ , and  $F$ , it is more likely that this treatment changes the surface rather than the bulk. Furthermore, since in going from state  $A$  to  $B$  to  $C$ , only the surface is affected, and the results cannot be explained if the SPV were to give the band bending, it would be very surprising if a different explanation were to hold in this case.



These results are in agreement with the observations of Abelson and de Rosny,<sup>12</sup> who measured the effect of adsorbates on the surface potential in *a*-Si:H using a Kelvin probe. The hypothesis that under strong illumination, the bands should flatten and thus directly provide the contact potential from the Kelvin probe measurement, gave them "unreliable" results, so they had to "discard" it.

#### D. Temperature dependence

Yamagishi<sup>21</sup> has measured the temperature dependence of SPV in *c*-Si (111) surfaces having a silicon-dioxide or a silicon-nitride layer. In both cases, SPV decreases linearly with temperature and becomes zero at higher temperatures. By assuming that the high-intensity SPV measures the surface potential, his results could be explained in terms of the shift of the Fermi level in the bulk as a function of temperature.

In the case of *a*-Si:H the observed variation of SPV with temperature is quite different than that of *c*-Si. SPV at the front surface decreases linearly but it changes sign as the temperature is raised instead of approaching zero as in *c*-Si with an oxide layer.<sup>21</sup> The temperature dependence of SPV at the back surface is even more puzzling. It increases initially, shows maximum at about  $T = 350$  K, and then decreases linearly at high temperatures. It has been shown in Sec. IV that the SPV in *a*-Si:H does not give surface potential and is determined mainly by the extent of participation of surface states by changing  $Q_{sc}$  ( $\Delta Q_{sc} = -\Delta Q_{ss}$ ). Hence the analysis of Yamagishi<sup>21</sup> cannot be applied which starts with the assumption that no surface states participate in SPV.

In the present case, the behavior of SPV with temperature will depend upon the parameters of surface states, such as capture rates for electrons and holes and their separation from the Fermi level and the mobility edges.<sup>6,8</sup> In the absence of such information in *a*-Si:H, it is difficult to give a definite interpretation of the behavior of SPV with temperature. However, some general statements can be made. The temperature dependencies of SPV measured at the front and the back surface are different. In order to check if this difference is because of an oxide layer which may be present at the front but not at the back surface, the sample was etched in an attempt to reduce the oxide at the front. Upon etching, the SPV at room temperature was found to be about the same for the front and the back surface. However, the  $T$  dependence was still quite different for the two surfaces (see Fig. 6).

This difference in  $T$  dependence cannot be explained by a slowly growing oxide layer during the measurement of SPV at high  $T$  since the value of SPV at room temperature is reproducible after the heat cycle. Although the presence of a thin oxide layer is expected to be present at the surface even after etching, the results seem to suggest that the difference between the front and the back surface states is not merely because of an oxide present at the front. This is not surprising, since in any case, the front surface is in vacuum and the back is in contact with the substrate resulting in different surface state parameters at the front and the back. Also, the plasma chemistry of silane in the beginning of the glow discharge may be different than at the end during the prepara-

tion, thus resulting in a different material and the back and the front.<sup>9</sup>

Other experiments<sup>24,25</sup> have also indicated different behavior of the front and the back surface space-charge layers. Transient photoconductivity and charge collection experiments on Cr/*a*-Si:H/Cr sandwich geometry by Sreet<sup>25</sup> indicate a very different behavior at the two surfaces. A possible explanation is that the initial deposition of *a*-Si:H yields material with a high defect density and the presence of an oxide layer and adsorbates affect the front surface, resulting in different surface state parameters for the front and the back surface.

## VI. LIGHT SOAKING AND SPV

### A. Experimental results

Although it is difficult to infer the band bending in *a*-Si:H from SPV, we shall show that it is possible to find out, whether light soaking (Staebler-Wronski effect) changes the surface or not by performing the following experiment.<sup>12</sup> Conductance ( $G$ ) and SPV are measured in different states of *a*-Si:H samples, obtained by exposing the heat-dried sample to a sequence of light soaking and moisture and then in the reverse sequence in a similar fashion to the experiment by Tanielian<sup>15</sup> in which he measured only  $G$ . Procedure of this experiment will be clear from Fig. 8.

Figure 8 shows the changes in  $G$  observed for an undoped sample of *a*-Si:H (No. 185) as a function of time as the surface conditions are changed.  $A$  represents the heat-dried state of the sample with  $G = 3.8 \times 10^{-13} \Omega^{-1}$ . At time  $t = 0$ , it is exposed to a white light (intensity 60 mW/cm<sup>2</sup>).  $G$  increases to  $1.2 \times 10^{-9} \Omega^{-1}$  in the presence of light, but then decreases slightly with time, reaching  $7.5 \times 10^{-10} \Omega^{-1}$  in 6 h (see Fig. 8, Cycle I). At  $t = 6$  h, the light is switched off and we obtain the light-soaked state  $B$ , which has a smaller  $G = 2.8 \times 10^{-13} \Omega^{-1}$ . Now the sample is exposed to moist nitrogen (relative humidity  $\approx 50\%$ ). In the presence of moisture,  $G$  first increases to  $6 \times 10^{-13} \Omega^{-1}$  and then slowly decreases in about 3 h to  $4.5 \times 10^{-13} \Omega^{-1}$  (state  $F$ ). For the reverse sequence (Fig. 8, Cycle II) the sample is again heat

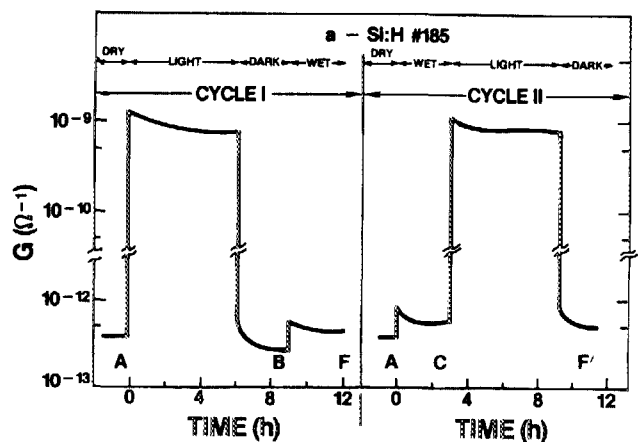


FIG. 8. Conductance ( $G$ ) as a function of time in the light-soaking moisture cycle experiment for an *a*-Si:H sample (No. 185).  $A$ : heat-dried state;  $B$ : light-soaked state;  $F$ : state  $B$  in presence of moisture;  $C$ : state  $A$  in presence of moisture;  $F'$ : state  $C$  after light soaking.

dried. After heat drying, the sample conductance comes back to state *A*. The heat-dried sample is exposed to moisture. *G* immediately increases to  $8.5 \times 10^{-13} \Omega^{-1}$  and then decreases (within about 3 h) to  $5.6 \times 10^{-13} \Omega^{-1}$  in equilibrium (state *C*). Now the sample is exposed to white light as before. The photoconductance reduces from  $1.05 \times 10^{-9} \Omega^{-1}$  to  $8 \times 10^{-10} \Omega^{-1}$  in 6 h. The final conductance in dark (state *F'*) is  $4.7 \times 10^{-13} \Omega^{-1}$ . These results agree qualitatively with those of Tanielian, and can be explained in a similar fashion<sup>15</sup> although the changes in *G* are much larger in his case.

The equilibrium value of *G* in each state is shown in the upper half of Fig. 9 for each of the cycles. The lower part of the figure shows SPV, measured with the high-energy (3 eV) and the band-gap light (1.8 eV), in different equilibrium states of the sample. In Fig. 10, results obtained on another undoped (sample No. 184, solid lines) and after doping it lightly with lithium (broken lines) are given. The variation of *G* and SPV in different states shows a trend similar to that shown in Fig. 9.

The first part of Fig. 11 gives the effect of light soaking on SPV and *G* on a sample (No. 186) before etching. States *A'* and *B'* represent the heat-dried and the light-soaked states, respectively, and their *G* and SPV values show a trend similar to other nonetched samples (Figs. 9 and 10). The sample in state *A'* is etched and heat dried to obtain the state *A*. The sample in state *A* is subjected to the light-soaking moisture cycles as before (see Fig. 11). On comparing the results on different samples in the cycle experiment, the following features are observed.

(1) SPV is positive in all states of all the samples. This

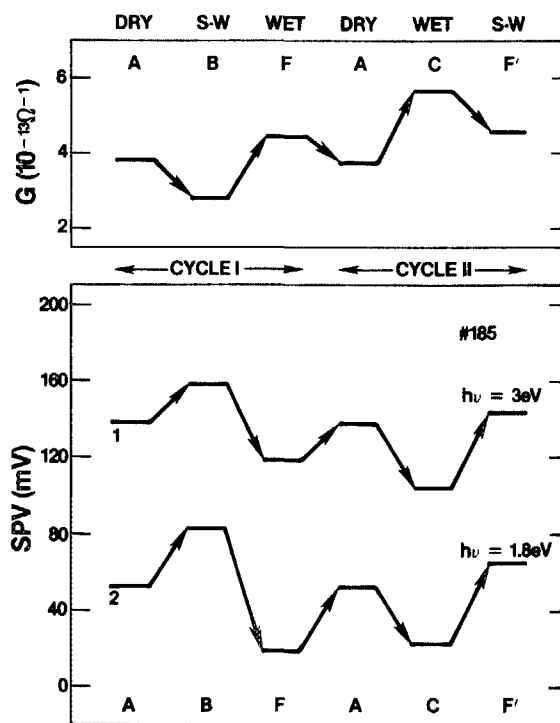


FIG. 9. *G* and SPV for sample No. 185 in different states of the cycle experiment. *G* is in upper half of the figure and SPV in the lower half. SPV curve 1 is for high-energy light  $E_2 \approx 3.0$  eV and Curve 2 is for optical gap light  $E \approx 1.8$  eV.

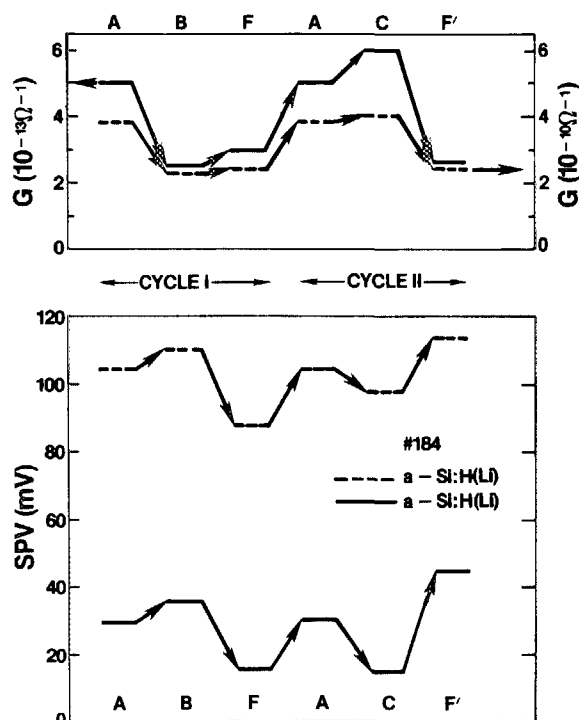


FIG. 10. *G* and SPV for an undoped *a*-Si:H sample (No. 184) and lightly Li-doped *a*-Si:H (Li) sample in different states of cycle experiment. SPV is for optical gap light  $E_1 \approx 1.8$  eV.

positive sign is in agreement with the literature.<sup>10,11</sup>

(2) The change in *G* upon exposure to moisture is larger for the heat-dried samples as compared to the light-soaked ones, in agreement with Tanielian.<sup>15</sup>

(3) Moisture increases *G* and decreases SPV.

(4) SPV is larger for the nonetched sample. This is in agreement with Aker *et al.*<sup>11</sup>

(5) Light soaking decreases *G* in all states of the samples, but its effect on SPV depends on whether the surface is etched or not. It (light soaking) increases SPV on the non-etched surface and decreases it (SPV) on the etched surface.

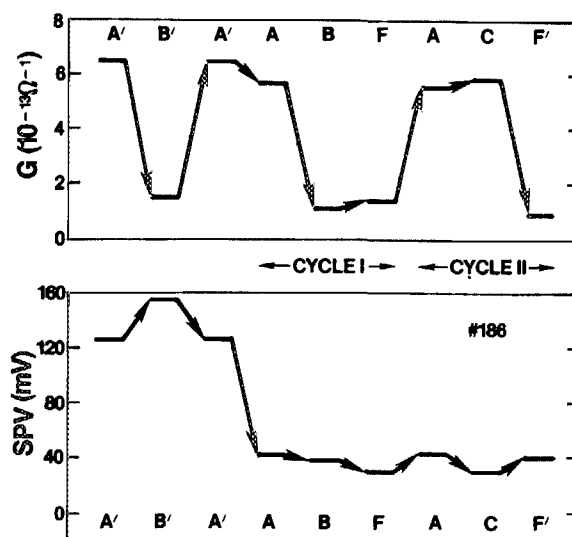


FIG. 11. *G* and SPV for an etched *a*-Si:H sample (No. 186) in different states of the cycle experiment. *A'*: nonetched, heat-dried state; *B'*: nonetched, light-soaked state; *A*-*F'* states are the same as in the cycle experiment.

Similar effect of etching on the change in SPV upon light soaking have also been observed by Aker *et al.*<sup>11</sup>

(6)  $G$  in states  $F$  and  $F'$  is almost the same (in agreement with Tanielian<sup>15</sup>). SPV in the state  $F'$  is always more than in state  $F$ .

(7) There is no correlation between the change in conductance  $\Delta G$  and the change in SPV from one state to another if we assume that the saturated value of SPV gives the magnitude and the direction of surface potential.<sup>11</sup> This is in agreement with the results already discussed in Sec. IV.

## B. Discussion

Water acts as a donor on the surface of many crystalline semiconductors and creates a band bending by causing a charge transfer between the adsorbed  $H_2O$  and the semiconductor.<sup>7</sup> This band bending creates an accumulation layer adjacent to the surface. Moisture ( $H_2O$ ) increases the conductance upon adsorption in the case of the intrinsic and  $n$ -type samples.<sup>1</sup> Increase of  $G$  upon exposure to moisture (states  $C$  and  $F$ ) support this view.

The observation by Tanielian<sup>15</sup> that  $G$  decreases upon exposure to moisture for  $p$ -type  $a$ -Si:H is a further indication that the observed changes in  $G$  are indeed caused by a change in the surface potential. Also, using adsorbates which are electron acceptors (e.g.,  $O_2$  and evaporated Se) it has been shown that  $G$  decreases in  $n$ -type  $a$ -Si:H as expected.<sup>15</sup> We also observed a decrease in  $G$  upon evaporation of a layer of Se onto undoped  $a$ -Si:H (which is slightly  $n$ -type) by a factor of about 10 for a 1- $\mu$ m-thick sample.

If light soaking increases the density of states around the Fermi level in the undoped specimen, the magnitude of the change in  $G$  upon exposure to moisture is expected to reduce. This is indeed observed in all cases, in agreement with Tanielian.<sup>15</sup> He points out that the observation that  $G(F) \simeq G(F')$  is also consistent with the hypothesis that light soaking affects the bulk states.

There is considerable debate in the literature about the origin of the change in  $G$  upon light soaking. Although we observe a decrease, an increase in  $G$  upon light soaking is also sometimes observed.<sup>25</sup> Whereas there is a lot of evidence to suggest that this is a bulk effect,<sup>27</sup> as assumed by Tanielian, the experiments of Solomon<sup>22</sup> and Hack and Madan<sup>28</sup> suggest that the light exposure affects the surface also. Hauschildt *et al.*<sup>29</sup> measured conductivity and thermopower before and after light soaking and concluded that they cannot be explained in terms of surface changes alone. More recently, using the Kelvin probe method, Abelson and de Rosny<sup>12</sup> found a reduction in band-bending variation under water adsorption. They interpreted this in terms of light-induced modification of the surface of  $a$ -Si:H.

Let us now turn our attention to the SPV results. The magnitude of change in  $G$  implies that the surface potential in states  $C$  and  $F$  in Figs. 9–11 must be negative (see Sec. IV). If SPV were to give the surface potential (as is usually the case in many crystals), one would expect a negative SPV in states  $C$  and  $F$ . But the observations are opposite. Furthermore, the decrease in  $G$ 's not always accompanied by an increase in SPV as observed after light soaking on the etched surfaces ( $A \rightarrow B$ , Fig. 11).

Aker *et al.*<sup>11</sup> have explained changes in  $G$  in boron-doped  $a$ -Si:H after light soaking by assuming bulk changes and by an increase in metastable charged defects within the oxide layer at the surface. The difference in SPV in change of state  $A' \rightarrow B'$  and  $A \rightarrow B$  (see Fig. 11, also remarks in Sec. VI A) may be due to an increase in metastable charges within the oxide layer and this may be less on the etched surface having a thinner layer of oxide. These observations provide further support for the conclusion already reached in Sec. V that SPV cannot be directly correlated with the surface potential in  $a$ -Si:H. However, even in this unfavorable situation, it can be concluded that light soaking changes the surface as well as the bulk, as follows. For the sake of argument, let us assume that light soaking changes the bulk states alone. Since the moisture affects only the surface, we should expect the same SPV in states  $F$  and  $F'$ , which is contrary to the observations. This should especially hold for the sample No. 184, whose activation energy does not change upon light soaking.

We are therefore led to conclude that light soaking changes the surface as well as the bulk states.

## VII. CONCLUSIONS

A relation between the space-charge density and the surface potential of  $a$ -Si:H has been derived under reasonable assumptions by solving Poisson's equation. It shows that in  $a$ -Si:H a negligible SPV is expected if the space-charge density were to remain unchanged upon shining light. A finite SPV can be observed only if there is a transfer of charge from the surface states into the space-charge region. In the latter case, however, the saturated value of SPV (measured at the highest intensity of light) may not be equal to the surface potential.

These theoretical considerations are helpful in understanding why various authors have encountered difficulties (when the measured SPV is interpreted as being equal to the surface band bending) in  $a$ -Si:H.<sup>11–13</sup> In the present study, the conductance and SPV measurements under different conditions show that SPV in  $a$ -Si:H does not give the band bending at the surface, and may even be of a sign opposite to what is normally expected. The frequency and temperature dependence also support this conclusion, which is in agreement with the theoretical arguments presented here. The results can be understood if the density of surface states responsible for SPV is taken to be about  $10^{11} \text{ cm}^{-2}$ , a number which appears quite reasonable. Furthermore, the frequency dependence of SPV shows that most of these states have time constants lying between 1 s and 1 ms.

Finally, by exposing  $a$ -Si:H to cycles of moisture and light soaking (Staebler–Wronski effect) and measuring SPV in addition to dark conductance,<sup>13,15</sup> it has been argued that light soaking changes the surface as well as the bulk of the film. Light soaking is known to create metastable centers in the bulk, which are believed to be dangling bonds that have a positive correlation energy.<sup>30</sup> There are, however, several experiments in the literature<sup>12,13,22,28,29</sup> which suggest that light soaking affects the surface also. The present work provides further evidence that in addition to changing the bulk, light soaking changes the surface as well.

## ACKNOWLEDGMENTS

We thank Professor R. Sharan, Dr. A. Mookerjee, Dr. A. Kumar, Dr. M. Hack, and Mr. D. S. Misra for many helpful discussions. This work is supported by a grant from the Department of Science and Technology (SERC), India.

- <sup>1</sup>W. H. Brattain and J. Bardeen, *Bell Syst. Tech. J.* **32**, 1 (1953).
- <sup>2</sup>E. O. Johnson, *Phys. Rev.* **111**, 153 (1958).
- <sup>3</sup>C. G. B. Garrett and W. H. Brattain, *Phys. Rev.* **99**, 376 (1955).
- <sup>4</sup>V. M. Buimistrov, A. P. Garbon, and V. G. Litovchenko, *Surf. Sci.* **3**, 445 (1965).
- <sup>5</sup>J. Lagowski, C. L. Balestra, and H. C. Gatos, *Surf. Sci.* **27**, 547 (1971).
- <sup>6</sup>D. L. Lile, *Surf. Sci.* **34**, 337 (1973).
- <sup>7</sup>A. Many, Y. Goldstein, and N. B. Grover, *Semiconductor Surfaces* (North-Holland, Amsterdam, 1965).
- <sup>8</sup>D. R. Frankl and E. A. Ulmer, *Surf. Sci.* **6**, 115 (1966).
- <sup>9</sup>H. Fritzsche, in *Semiconductor and Semimetals, Vol. 21C: Electronic and Transport Properties of Hydrogenated Amorphous Silicon*, edited by J. I. Pankove (Academic, New York, 1984), p. 309.
- <sup>10</sup>B. Goldstein and D. J. Szostak, *Surf. Sci.* **99**, 235 (1980).
- <sup>11</sup>B. Aker, Shao-Qi Peng, Song-yi Cai, and H. Fritzsche, *J. Non-Cryst. Solids* **59&60** 509 (1983).
- <sup>12</sup>J. Abelson and G. de Rosny, *J. Phys. (Paris)* **44**, 993 (1983).
- <sup>13</sup>S. Kumar and S. C. Agarwal, *Philos. Mag.* **B 49**, L53 (1984); S. Kumar and S. C. Agarwal, *Appl. Phys. Lett.* **45**, 575 (1984).
- <sup>14</sup>D. L. Staebler and C. R. Wronski, *Appl. Phys. Lett.* **31**, 292 (1977); *J. Appl. Phys.* **51**, 3261 (1980).
- <sup>15</sup>M. Tanielian, *Philos. Mag.* **B 45**, 435 (1982).
- <sup>16</sup>A. Madan, P. G. LeComber, and W. E. Spear, *J. Non-Cryst. Solids* **20**, 239 (1976).
- <sup>17</sup>D. S. Misra, Ph. D. Thesis, I. I. T. Kanpur (1984) (unpublished).
- <sup>18</sup>W. Shockley and W. T. Read, *Phys. Rev.* **87**, 835 (1952).
- <sup>19</sup>J. G. Simmons and G. W. Taylor, *Phys. Rev. B* **4**, 502 (1977).
- <sup>20</sup>T. Tiedje, *Appl. Phys. Lett.* **40**, 627 (1982).
- <sup>21</sup>H. Yamagishi, *J. Phys. Soc. Jpn.* **25**, 766 (1968).
- <sup>22</sup>I. Solomon, T. Ditl, and D. Kaplan, *J. Phys. (Paris)* **39**, 1241 (1978).
- <sup>23</sup>C. E. Reed and C. G. Scott, in *Surface Physics of Phosphors and Semiconductors*, edited by C. G. Scott and C. E. Reed (Academic, New York, 1975).
- <sup>24</sup>P. G. LeComber, W. E. Spear, R. A. Gibson, H. Mannsperger, and F. Djamdji, *J. Non-Cryst. Solids* **59&60**, 505 (1983).
- <sup>25</sup>R. A. Street, *Phys. Rev. B* **27**, 4924 (1983).
- <sup>26</sup>H. Mell and W. Beyer, *J. Non-Cryst. Solids* **59&60**, 405 (1983).
- <sup>27</sup>D. Adler, *Solar Cells* **9**, 133 (1983).
- <sup>28</sup>M. Hack and A. Madan, *Appl. Phys. Lett.* **41**, 272 (1982).
- <sup>29</sup>D. Hauschildt, W. Fuhs, and H. Mell, *Phys. Status Solidi B* **111**, 171 (1982).
- <sup>30</sup>H. Fritzsche, in *Proceedings of the International Topical Conference on Optical Effects in Amorphous Semiconductors*, Aug. 1-4, 1984, Snowbird, Utah, AIP Conf. Proc. **120**, 478 (1984).